

Received January 7, 2021, accepted January 8, 2021, date of publication January 13, 2021, date of current version January 22, 2021.

Digital Object Identifier 10.1109/ACCESS.2021.3051351

Two-Stage Joint Optimal Scheduling of a Distribution Network With Integrated Energy Systems

YUHAN JIANG¹, FEI MEI¹, (Member, IEEE), JIXIANG LU², AND JINJUN LU²

¹College of Energy and Electrical Engineering, Hohai University, Nanjing 211100, China

²State Key Laboratory of Smart Grid Protection and Control, NARI Group Corporation, Nanjing 211000, China

Corresponding author: Fei Mei (meifei@hhu.edu.cn)

This work was supported in part by the State Key Laboratory of Smart Grid Protection and Control (SKL of SGPC), and in part by the National Key Research and Development Program of China under Grant 2018YFB0905000 and Grant SGTJDK00DWJS1800232.

ABSTRACT The coordinated operation of an integrated energy system (IES) and a distribution network is the inevitable development trend of the energy Internet of the future. The day-ahead optimal scheduling of the IES is an important way to improve new energy efficiency and the energy economy. When the IES and the distribution network exchange electrical energy, the voltage of the distribution network may be out of limit. This article presents a two-stage joint optimal scheduling method for a distribution network with IESs to improve the economy of the IESs and the safety of the distribution network. In the first stage, the user's demand response and the electrical energy interaction between IESs are considered, and the schedulable potential of the systems is fully tapped. In the second stage, a bi-level scheduling model is adopted: the upper model takes the distribution network as the control object and reduces the power loss by adjusting the exchange power between the distribution network and the IESs. The lower model takes the IESs as the control objects and obtains the scheme with the lowest cost in each IES through multi-objective particle swarm optimization. Taking the IEEE 33-node distribution system as an example, simulation research is performed to show that the total network loss is 17.01% lower and the total cost is 5.36% lower than the method without two-stage optimal scheduling, which verifies the effectiveness of the proposed method.

INDEX TERMS Integrated energy system (IES), joint optimal scheduling, power interaction, bi-level scheduling model.

I. INTRODUCTION

Energy is an indispensable resource for human productivity and life, and it is an important material basis for the national economy. To avoid excessive exploitation of fossil energy such as coal and oil, making full use of renewable energy has become an inevitable development trend of the power industry [1], [2]. In recent years, China's renewable energy related technologies have developed rapidly. According to the National Energy Administration, China's installed capacity for renewable energy generation reached 794 million kW by the end of 2019, accounting for 39.5% of the country's total installed power capacity. However, with wind power, photovoltaic energy and other renewable energy in the form of distributed energy in the power grid access, most renewable

energy has an obvious randomness and intermittency, which brings great hidden trouble to the safe and stable operation of the power system. It is necessary to adopt certain methods to improve the energy efficiency and ensure the reliable operation of the power system [3]. In this context, the integrated energy system (IES) under the fusion of a smart grid and energy network came into being [4]. The IES can effectively convert electricity, gas, heat, cold and other forms of energy in the energy hub to dynamically meet the energy needs of different users. On the other hand, the IES can make full use of renewable energy on the energy supply side, accomplish local consumption of renewable energy, and improve energy efficiency. At the same time, fully exploiting the schedulable potential of the IES can provide a certain reserve capacity for the distribution network, play the role of load shifting, and improve the security of the distribution network.

The associate editor coordinating the review of this manuscript and approving it for publication was Amjad Anvari-Moghaddam¹.

For research of the schedulable potential, [5] proposed that the schedulable potential of a controllable load could be obtained from the difference between the original load curve and the average daily load curve of the coolest N days in summer. Reference [6] proposed that the length of air conditioning shutdown time can reflect the size of the schedulable potential. References [7], [8] introduced the power supply capacity index to quantify the schedulable potential of electric vehicles and other schedulable resources. The main factors affecting the power supply capacity include the remaining synchronization time and the scheduling capacity at the current moment.

There have been many studies on the optimal scheduling model of the IES. Reference [9] established a multi-objective capacity planning model with the minimum energy and environmental cost as the objective function. Reference [10] proposed a modified crisscross particle swarm optimization-surrogate worth trade-off (MCPSO-SWT) solution methodology to search for the best non-dominated solution and analyze the impact of renewable energy sources in terms of cost and emission. Reference [11] optimized the distributed energy system to minimum the total cost and pollution by the multi-objective algorithm. Reference [12] proposed an optimization operation method of a regional integrated energy system (RIES) based on repeated game. The distribution network selected the power loss and load equilibrium rate of the distribution network as the bi-objective, and the micro-energy network selected the daily operating cost as the objective function for conducting repeated game to realize the coordinated economic optimization operation of the RIES. Reference [13] proposed a two-stage multi-objective scheduling method consisting of a multi-objective optimal power flow calculation and multi-attribute decision making stages. Reference [14] considered the influence of renewable energy on the power of a distribution network and improved the flexibility of the system through the regulation capacity of central air conditioning and a district heating system. Reference [15] proposed an optimal coordination control strategy of hybrid energy storage systems to prevent power fluctuations of the tie-line in integrated community energy systems (ICESs). Reference [16] established the distribution network and natural gas network models and proposed the coordinated operation and optimal scheduling method for the combined gas-electricity distribution network. Reference [17] established a hierarchical multi-objective fuzzy cooperative optimization scheduling model. The upper layer was a multi-energy flow calculation of power system, natural gas system and thermal system, while the lower layer was a multi-objective model considering operation cost, renewable energy consumption, pollution emission and fossil energy consumption. Reference [18] proposed a novel two-stage stochastic scheduling of probabilistic approach and established a model with IESs, distribution grid and natural gas system to improve the economy of the system. References [19], [20] proposed a demand response mechanism that considered the electricity load and thermal load and constructed a multi-time

scale optimal scheduling model and a multi-objective optimal scheduling model, respectively.

In sum, most of the literature focuses on studying the schedulable potential primarily for two types of flexible loads, the temperature-controlled load and the electric vehicle, and the schedulable potential of the IES has not been discussed. Studies on the optimal scheduling of the IES focus on the internal economy of the IES, ignoring the possible effect of energy exchange between the IES and the distribution network on the safety of the distribution network.

The research in this article is based on previous studies. In contrast, the contributions and innovations of this article are as follows:

- 1) Taking the integrated energy system and distribution network as research objects, the interests of both parties are taken into account, not only the economic efficiency and emission targets of the integrated energy system.
- 2) In the existing studies, the research objects of the schedulable potential are usually temperature-controlled loads and electric vehicles. In this article, the research object of the schedulable potential is extended to the integrated energy system, and the schedulable potential of the integrated energy system is defined as the maximum output of the integrated energy system as an equivalent power source.
- 3) This article primarily proposes a two-stage joint optimal scheduling strategy for a distribution network with IESs. In the first stage, the schedulable potential of the IESs is fully tapped by considering the demand response on the user side; in the second stage, the schedulable potential is taken as the exchange power constraint between the IESs and the distribution network, and a bi-level optimal scheduling model is established. The upper level is a distribution network model considering security constraints, and the lower level is a multi-objective optimal scheduling model considering the economics of multiple IESs. The solution is obtained using the multi-objective particle swarm optimization algorithm. An example of the IEEE 33-node distribution system combined with park-level integrated energy systems is presented to demonstrate the effectiveness of the proposed optimal scheduling model.

II. STRUCTURE OF A DISTRIBUTION NETWORK WITH IESS AND THE MATHEMATICAL MODELS OF EQUIPMENT

A. STRUCTURE OF THE IES

The combined cooling, heating and power (CCHP) system includes four forms of energy: cold, heat, electricity and gas. In this article, a typical CCHP system is taken as the research object. The study area is located inland, the wind power generation is less and the photovoltaic power generation is large, so only the renewable energy photovoltaic is added to the CCHP system. Figure 1 shows the basic IES structure. The system consists of the photovoltaic, gas turbines, waste heat recovery system, gas boiler, heat exchanger, electric

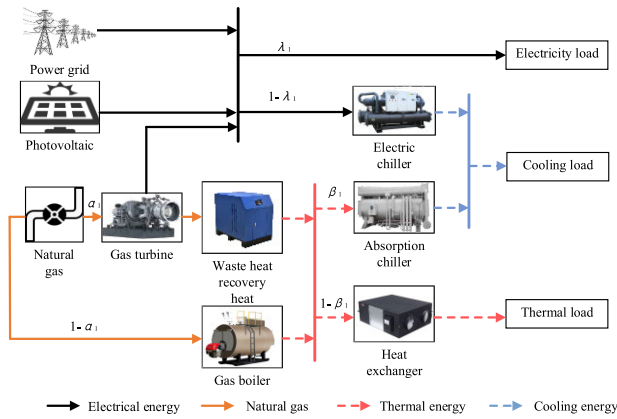


FIGURE 1. Structure of an IES.

chiller and absorption chiller. Among these energy sources, electrical energy is primarily provided by the power grid, photovoltaic and gas turbine and is used to meet the electrical energy demand of the users and the power demand of the electric chiller. The thermal energy is primarily provided by the waste heat recovery system and gas boiler and is used to meet the thermal load demand of the users and the thermal energy demand of the absorption chiller. The cooling energy is primarily provided by the electric chiller and absorption chiller to meet the cooling needs of the users. α_1 , β_1 and λ_1 are the scaling factors of natural gas distribution to the gas turbine, the thermal energy distribution to the absorption chiller and the electrical energy distribution to the electricity load, respectively.

B. STRUCTURE OF A DISTRIBUTION NETWORK WITH IESS

The structure of a distribution network with IESs is shown in Figure 2. The system contains a distribution network and multiple IESs. Among them, the IES acts as the equivalent power source and the equivalent load of the distribution network. The power exchange between the distribution network and the IES can be performed, and the power interaction between the park-level integrated energy systems can also be performed through the tie line.

The joint scheduling strategy of the distribution network and the IESs is as follows: when photovoltaic and gas turbine electricity generation in an IES cannot meet the IES's power demand, the IES has the priority to purchase electricity from other IESs that have extra electricity, and the other IESs can consider whether to sell electricity to the power-shortage IES. If the shortage of electricity persists, then purchasing electricity from the grid is considered. When the photovoltaic and gas turbine electricity generation in an IES is in surplus, and there is still more power after meeting the power demands

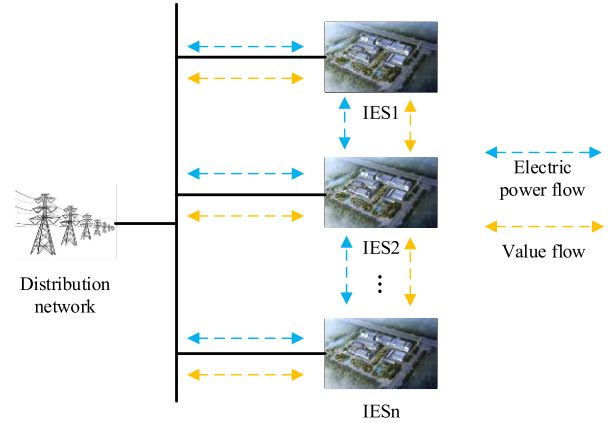


FIGURE 2. Structure of a distribution network with IESs.

of the users and the electrical equipment in the IES, the IES will consider whether to sell electricity to the power-shortage IESs and the power grid.

C. MODELLING THE EQUIPMENT OF AN IES

1) ENERGY HUB MODEL

The Swiss Federal Institute of Technology in Zurich first proposed the concept of the energy hub [21]. The energy hub has been widely applied in optimal scheduling, optimal design and other fields [22], [23]. The energy hub is an important part of an IES that can transform, distribute and store various types of energy [24], [25]. The expression for the energy hub model in this article is as follows (1), as shown at the bottom of the page, where L_e , L_h and L_c are the electricity load, thermal load and cooling load, respectively; P_e , P_g and P_{pv} are the energy input of the power grid, natural gas and photovoltaic, respectively; η_t , η_{gt}^e , η_{gt}^h , η_{rec} , η_{gb} , η_{ex} , η_{ec} and η_{ac} are the transformer efficiency, gas turbine electrical efficiency, gas turbine thermal efficiency, waste heat recovery system efficiency, gas boiler efficiency, electric chiller efficiency and absorption chiller efficiency, respectively.

2) GAS TURBINE MODEL

A gas turbine is a common power generator in an IES. The high-temperature waste heat flue gas discharged during power generation can accomplish heating through the waste heat recovery system. Its mathematical model is as follows:

$$P_{gt}(t) = G_{gt}(t)\eta_{gt}^e(t), \quad t = 1, 2, \dots, 24 \quad (2)$$

$$\eta_{gt}^e(t) = a\left(\frac{P_{gt}(t)}{P_{N,gt}}\right)^3 + \beta\left(\frac{P_{gt}(t)}{P_{N,gt}}\right)^2 + \gamma\left(\frac{P_{gt}(t)}{P_{N,gt}}\right) + \mu, \quad t = 1, 2, \dots, 24 \quad (3)$$

$$\eta_{gt}^h(t) = 1 - \eta_{gt}^e(t) - \eta_{loss}(t), \quad t = 1, 2, \dots, 24 \quad (4)$$

$$\begin{bmatrix} L_e \\ L_h \\ L_c \end{bmatrix} = \begin{bmatrix} \eta_t \lambda_1 & \eta_{gt}^e \alpha_1 \lambda_1 & \lambda_1 \\ 0 & (\eta_{gt}^h \eta_{rec} \alpha_1 + \eta_{gb}(1 - \alpha_1)) \eta_{ex} (1 - \beta_1) & 0 \\ \eta_t \eta_{ec} (1 - \lambda_1) & \eta_{gt}^e \eta_{ec} \alpha_1 (1 - \lambda_1) + \eta_{gt}^h \eta_{rec} \eta_{ac} \alpha_1 \beta_1 + \eta_{gb} \eta_{ac} (1 - \alpha_1) \beta_1 & (1 - \lambda_1) \end{bmatrix} \begin{bmatrix} P_e \\ P_g \\ P_{pv} \end{bmatrix} \quad (1)$$

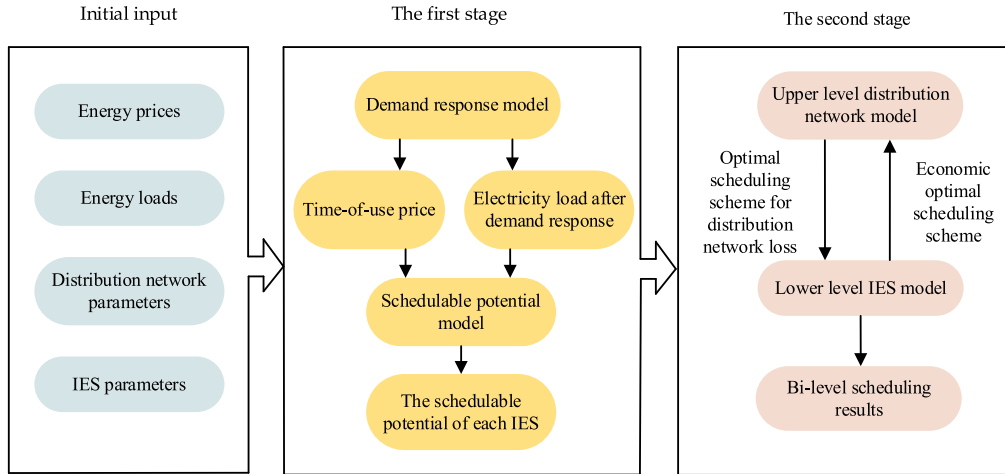


FIGURE 3. Strategy of two-stage optimal scheduling.

$$Q_{gt}(t) = P_{gt}(t)(1 - \eta_{gt}^e(t) - \eta_{loss}(t))/\eta_{gt}(t), \quad t = 1, 2, \dots, 24 \quad (5)$$

where $P_{gt}(t)$ is the electric power of the gas turbine at time t ; $G_{gt}(t)$ is the consumption of natural gas at time t ; $\eta_{gt}^e(t)$ is the electric efficiency of the gas turbine at time t ; $P_{N,gt}$ is the rated electric power; and α , β , γ and μ are the gas turbine power generation output coefficients. $\eta_{gt}^h(t)$ and $\eta_{loss}(t)$ are the output thermal efficiency and thermal loss rate of the gas turbine at time t , respectively. $Q_{gt}(t)$ is the heat output power of the gas turbine at time t .

3) GAS BOILER MODEL

The gas boiler produces heat primarily by consuming natural gas. Its mathematical model is as follows:

$$Q_{gb}(t) = \eta_{gb}(t)G_{gb}(t), \quad t = 1, 2, \dots, 24 \quad (6)$$

where $Q_{gb}(t)$ and $G_{gb}(t)$ are the thermal output and the consumption of natural gas at time t , respectively. $\eta_{gb}(t)$ is the heating efficiency of the gas boiler at time t .

4) ELECTRIC CHILLER MODEL

The electric chiller primarily liquefies the refrigerant gas through mechanical pressure and makes use of its characteristic of liquefaction and heat absorption to accomplish refrigeration. Its mathematical model is as follows:

$$Q_{ec}(t) = COP_{ec} \cdot P_{ec}(t), \quad t = 1, 2, \dots, 24 \quad (7)$$

where $Q_{ec}(t)$ is the output cooling power of the electric chiller at time t ; COP_{ec} is the refrigeration coefficient, that is, the ratio of input electrical energy to output cooling energy; and $P_{ec}(t)$ is the electric power input by the electric chiller at time t .

5) ABSORPTION CHILLER MODEL

The absorption chiller drives the equipment to be converted into cold energy output by the input of heat energy, and its

mathematical model is as follows:

$$Q_{ac}(t) = COP_{ac} \cdot Q_{ac}^H(t), \quad t = 1, 2, \dots, 24 \quad (8)$$

where $Q_{ac}(t)$ is the output cooling power of the absorption chiller at time t ; COP_{ac} is the ratio of input electrical energy and output cooling energy of the absorption chiller; and $Q_{ac}^H(t)$ is the thermal power required to drive the absorption chiller at time t .

III. TWO-STAGE JOINT OPTIMAL SCHEDULING

Considering the safety of the distribution network and the economy of the IESs, this article proposes a two-stage optimal scheduling strategy that considers the schedulable potential of each IES, as shown in Figure 3. In the first stage, the schedulable potential of each IES is obtained through the input initial energy prices, initial energy loads, distribution network parameters and IES parameters; in the second stage, according to the schedulable potential of each IES obtained in the first stage, it is taken as the constrained condition for the exchange power between the distribution network and the IESs. The upper level distribution network will transfer the optimal scheduling scheme of distribution network loss to the lower level. In the lower level, according to the information transmitted by the upper level, if the distribution network transmits the power to the IES, it means the IES is short of power, and the IES will not transmit power to other IES. If the IES transmits power to the distribution network or the value of the exchange power is zero, the IES will transmit the power to other IES and the power is generated by the model randomly. The lower level IESs will transfer the economic optimal scheduling scheme to the upper level. After the iterations of the upper level model and the lower level model, the solutions of the upper and lower levels will be combined to obtain the optimal scheduling scheme that considers the distribution network loss and the economy of the park-level integrated energy systems.

A. SCHEDULABLE POTENTIAL CONSIDERING DEMAND RESPONSE

1) PRICE-BASED DEMAND RESPONSE MODEL

Price-based demand response refers to the behavior of the power supplier to set different electricity prices and the user to adjust the electricity demand according to the price signals received [26], [27]. The time-of-use price is the most widely used price type of demand response at present. The time-of-use price determines the three periods of peak, off-peak and valley based on the load, increases the electricity price in a peak period and reduces it in a trough period, effectively adjusts the user’s electricity consumption behavior, and accomplishes load shifting.

The user’s response to the electricity prices has been represented as [28], [29]:

$$\begin{bmatrix} \Delta q_f/q_f \\ \Delta q_p/q_p \\ \Delta q_g/q_g \end{bmatrix} = E \begin{bmatrix} \Delta p_f/p_f \\ \Delta p_p/p_p \\ \Delta p_g/p_g \end{bmatrix} \tag{9}$$

$$E = \begin{bmatrix} E_{ff} & E_{fp} & E_{fg} \\ E_{pf} & E_{pp} & E_{pg} \\ E_{gf} & E_{gp} & E_{gg} \end{bmatrix} \tag{10}$$

$$\begin{cases} E_{ii} = \frac{\Delta q_i/q_i}{\Delta p_i/p_i} \\ E_{ij} = \frac{\Delta q_i/q_i}{\Delta p_j/p_j} \end{cases} \tag{11}$$

where q_f , q_p and q_g are the total load during the peak period, off-peak period and valley period, respectively; Δq_f , Δq_p and Δq_g are the total load changes in the peak period, off-peak period and valley period, respectively; p_f , p_p and p_g are the electricity price of the peak period, off-peak period and valley period, respectively; Δp_f , Δp_p and Δp_g are the changes in electricity price in the peak period, off-peak period and valley period, respectively; E is the elasticity coefficient matrix of the electricity price. Each variable in the matrix is the elasticity coefficient of the electricity price, which is used to represent the user’s sensitivity to a multi-period electricity price. E_{ii} and E_{ij} are the self-elasticity coefficient and cross-elasticity coefficient, respectively; Δq_i , Δp_i and Δp_j are the variation of the electricity price and the electricity price in time period i and time period j , respectively; q_i , p_i and p_j represent the electric quantity and the change in the electricity price in time period i and the electricity price in time period j , respectively.

At the same time, according to the users’ satisfaction with the electricity usage and electricity expense, two constraint indexes are proposed, namely, the users’ satisfaction with electricity usage and the users’ satisfaction with electricity expense:

$$S_m = 1 - \frac{\sum_{i=1}^{24} |\Delta q_i|}{\sum_{i=1}^{24} q_i} \tag{12}$$

$$S_p = 1 - \frac{\sum_{i=1}^{24} \Delta C_i}{\sum_{i=1}^{24} C_i} \tag{13}$$

where S_m and S_p are the satisfaction degree of the users’ electricity usage mode and electricity expense, respectively. Δq_i and q_i are the change in the electric quantity at time i and the electric quantity at time i , respectively. q_i is a positive value; ΔC_i and C_i are the change in the electric charge expenditure at time i and the electric charge expenditure at time i , respectively.

Therefore, the price-based demand response model can be expressed as:

$$\begin{aligned} \min & \left(\frac{\max q' - \min q'}{\max q - \min q} \right) \\ \text{s.t.} & \begin{cases} p'_g \leq p'_p \leq p'_f \\ \Delta q_f + \Delta q_p + \Delta q_g = 0 \\ S_m \geq \alpha \\ S_p \geq \beta \end{cases} \end{aligned} \tag{14}$$

where the objective function is the standardized peak-valley difference; q' and q are the electric quantity after and before demand response, respectively; p'_g , p'_p and p'_f are the electricity price in the valley period, off-peak period and peak period after demand response, respectively; and α and β are the constraint values of the user’s satisfaction with the electricity usage mode and the electricity expense, respectively.

2) SCHEDULABLE POTENTIAL MODEL

After the park-level integrated energy systems are connected to the distribution network, it is equivalent to the equivalent loads or equivalent power sources. For the distribution network, when the IESs purchase electricity from the grid, the IESs are equivalent to the equivalent loads. When the IESs sell electricity to the grid, the IESs are equivalent to the equivalent power sources.

The schedulable potential of the IESs is primarily considered to fully tap the maximum output of the IESs as equivalent power after the IESs participate in scheduling and under the condition of ensuring the safe operation of the distribution network. During the peak period of power consumption, maximize gas turbine output, reduce the power purchased from the grid while meeting the IESs’ power demand, and improve the IESs’ economy; during the valley period, users increase their electricity consumption through a price-based demand response, fully absorb renewable energy, and thus reduce power fluctuations. The schedulable potential of each IES is taken as the constrained condition of the power exchange between the distribution network and the IESs.

a: OBJECTIVE FUNCTION

The aim of research on the schedulable potential is to determine the maximum energy that can be supplied to the distribution network by the study IES as an equivalent power

source, and its expression is as follows:

$$F_1 = \min(P_{k,b}(t) - P_{k,GT}^{sell}(t) - P_{k,PV}^{sell}(t)), \quad t = 1, 2, \dots, 24 \quad (15)$$

where $P_{k,GT}^{sell}(t)$, $P_{k,PV}^{sell}(t)$ and $P_{k,b}(t)$ are the quantity of gas turbine power sales, photovoltaic power sales, and power purchased from the grid by the k th IES in time period t , respectively. A negative value of the schedulable potential means the IES sells electricity to the grid, while a positive value means the IES buys electricity from the grid.

b: CONSTRAINED CONDITION

i) DISTRIBUTION NETWORK VOLTAGE CONSTRAINTS

$$V_{i,\min} \leq V_i(t) \leq V_{i,\max}, \quad t = 1, 2, \dots, 24 \quad (16)$$

where $P_{k,ex}$ is the voltage of node i at time t , and $V_{i,\max}$ and $V_{i,\min}$ are the upper and lower limits of the voltage at node i , respectively. When the distribution network transmits power to the IESs, the voltages of some nodes may be lower than the lower limit of the voltage. When the IESs transmit power to the distribution network, the voltages of some nodes may exceed the upper limit.

ii) POWER EXCHANGE CONSTRAINT BETWEEN IESS

$$\begin{aligned} 0 &\leq P_{k,ex}(t) \leq P_{k,GT}(t) + P_{k,PV}(t) - P_{k,ereq}(t) \\ P_{k,ereq}(t) &= P_{k,load}(t) + P_{k,EC}(t), \quad t = 1, 2, \dots, 24 \end{aligned} \quad (17)$$

where $P_{k,ex}(t)$ is the electrical energy transmitted from the k th IES with excess power to power-shortage IESs at time t ; $P_{k,GT}(t)$, $P_{k,PV}(t)$ and $P_{k,ereq}(t)$ are the gas turbine power generation, photovoltaic power generation and equivalent electrical energy demand within the k th IES, respectively; and $P_{k,load}(t)$ and $P_{k,EC}(t)$ are the power demand of users in the k th IES and the power consumption of the electric chiller, respectively.

iii) OUTPUT OF EQUIPMENT CONSTRAINT

$$P_{\min}^n \leq P_n(t) \leq P_{\max}^n, \quad t = 1, 2, \dots, 24 \quad (18)$$

where $P_n(t)$ is the output of equipment in group n ; and P_{\max}^n and P_{\min}^n are the upper and lower limits of equipment output of group n , respectively.

iv) ENERGY BALANCE CONSTRAINT

$$\begin{aligned} P_{k,PV}(t) + P_{k,GT}(t) + P_{k,b}(t) + P_{k,exb}(t) - P_{k,exs}(t) - P_{k,s}(t) \\ &= P_{k,ereq}(t) \\ H_{k,GB}(t) + H_{k,HRS}(t) &= H_{k,ereq}(t) \\ H_{k,ereq}(t) &= H_{k,AC}(t) + H_{k,load}(t) \\ C_{k,AC}(t) + C_{k,EC}(t) &= C_{k,load}(t), \quad t = 1, 2, \dots, 24 \end{aligned} \quad (19)$$

where $P_{k,b}(t)$ and $P_{k,s}(t)$ are the purchase and sale of electricity from the grid in the k th IES in time period t , respectively; $P_{k,exb}(t)$ and $P_{k,exs}$ are the purchase and sale of electricity from the k th IES to other IESs in time period t ; $H_{k,GB}(t)$ and $H_{k,HRS}(t)$ are the heat power recovered by the gas boiler and waste heat recovery system in the k th IES in time period t , respectively; $H_{k,ereq}(t)$, $H_{k,AC}(t)$ and $H_{k,load}(t)$ are the equivalent thermal energy demand, heat consumption of the absorption chiller and the user's thermal energy demand of the k th IES in time period t , respectively; and $C_{k,AC}(t)$, $C_{k,EC}(t)$ and $C_{k,load}$ are the cooling power provided by the absorption chiller and electric chiller in the k th IES in time period t and the cooling energy demand of the users, respectively.

B. BI-LEVEL OPTIMAL SCHEDULING FOR DISTRIBUTION NETWORK MODEL

The day-ahead economic scheduling model constructed in this article includes two parts: the distribution network and the park-level integrated energy systems. To consider the interests of both sides of the distribution network and the IESs, the upper level distribution network is scheduled with the goal of minimum network loss, while the lower level IES is scheduled with the goal of minimum cost.

1) UPPER LEVEL DISTRIBUTION NETWORK SCHEDULING MODEL

a: OBJECTIVE FUNCTION

$$\begin{aligned} F_2 &= \min P_{loss} \\ P_{loss} &= \sum_{t=1}^T \sum_{k=1}^n \sum_{j \in i} G_{ij} [U_i^2(t) + U_j^2(t) - 2U_i(t)U_j(t) \cos \theta_{ij}(t)] \end{aligned} \quad (20)$$

$$t = 1, 2, \dots, 24 \quad (21)$$

where P_{loss} is the total network power loss; T is the operating period; n is the number of distribution network nodes; G_{ij} is the conductance between nodes i and j ; $U_i(t)$ and $U_j(t)$ are the voltage at nodes i and j at time t , respectively; and $\theta_{ij}(t)$ is the phase angle difference between nodes i and j at time t .

b: CONSTRAINED CONDITION

i) POWER FLOW CONSTRAINT [30]

$$\begin{cases} P_{Gi}(t) - P_{di}(t) = U_i(t) \\ \quad \times \sum_{j \in i} U_j(t) (G_{ij} \cos \theta_{ij}(t) + B_{ij} \sin \theta_{ij}(t)) \\ Q_{Gi}(t) - Q_{di}(t) = U_i(t) \\ \quad \times \sum_{j \in i} U_j(t) (G_{ij} \sin \theta_{ij}(t) - B_{ij} \cos \theta_{ij}(t)) \end{cases} \quad t = 1, 2, \dots, 24 \quad (22)$$

where $P_{Gi}(t)$, $P_{di}(t)$, $Q_{Gi}(t)$ and $Q_{di}(t)$ are the active power output, active load, reactive power output and reactive load at node i at time t , respectively.

ii) GENERATOR SET OUTPUT CONSTRAINT

$$\begin{cases} P_{Gi,\min} \leq P_{Gi}(t) \leq P_{Gi,\max} \\ Q_{Gi,\min} \leq Q_{Gi}(t) \leq Q_{Gi,\max} \end{cases}, \quad t = 1, 2, \dots, 24 \quad (23)$$

where $P_{Gi,\max}$ and $P_{Gi,\min}$ are the upper and lower level limits of the generator active power at node i , respectively; and $Q_{Gi,\max}$ and $Q_{Gi,\min}$ are the upper and lower level limits of reactive power of the generator at node i , respectively.

iii) THE POWER EXCHANGE BETWEEN THE DISTRIBUTION NETWORK AND IES CONSTRAINT

$$P_{i,\min} \leq P_{i,pcc}(t) \leq P_{i,\max}, \quad t = 1, 2, \dots, 24 \quad (24)$$

where $P_{i,pcc}(t)$ is the exchange power between the distribution network and the IES at node i at time t ; when $P_{i,pcc}(t)$ is negative, the IES transmits power to the distribution network; when $P_{i,pcc}(t)$ is positive, the distribution network transmits power to the IES; $P_{i,\min}$ is the schedulable potential at node i , that is, the maximum power transmitted from the IES to the distribution network; and $P_{i,\max}$ is the maximum value of electricity purchased from the IES by the distribution network at node i .

2) LOWER LEVEL IES SCHEDULING MODEL

a: OBJECTIVE FUNCTION

$$\begin{aligned} F_3 &= \min(C_1 + C_2 + C_3) \quad (25) \\ C_1 &= \sum_{t=1}^{24} [F_{GT}(P_{GT}(t)) + F_{GB}(P_{GB}(t))] \cdot C_{gass} \\ C_2 &= \sum_{t=1}^{24} \sum_{i=1}^n \alpha_i P_i(t) \\ C_3 &= \sum_{t=1}^{24} (c_{b1} P_{b1}(t) + c_{b2} P_{b2}(t) - c_{s1} P_{s1}(t) - c_{s2} P_{s2}(t)) \end{aligned}$$

$t = 1, 2, \dots, 24 \quad (26)$

where C_1 , C_2 and C_3 represent the fuel cost, equipment operating cost and interaction cost of the IES, respectively; F_{GT} and F_{GB} are the gas turbine (GT) and gas boiler (GB) consumption of natural gas in time period t , respectively; C_{gass} is the price of natural gas; α_i and $P_i(t)$ are the operation and maintenance cost of the equipment in group i and the output power in time period t , respectively; $P_{b1}(t)$ and c_{b1} are the power and price of purchasing electricity from the grid in time period t , respectively; $P_{b2}(t)$ and c_{b1} are the power and price of purchasing electricity from other IESs in time period t , respectively; $P_{s1}(t)$ and c_{s1} are the power and price of electricity sold to the grid in time period t , respectively; and $P_{s2}(t)$ and c_{s2} are the power and price of electricity sold to other IESs in time period t , respectively.

b: CONSTRAINED CONDITION

Constraints include power balance constraints, power exchange constraints between IESs and equipment output constraints, as shown in Equations (17) - (19).

C. MODEL SOLVING

In the upper optimization solution, the `fmincon` function in the MATLAB toolbox has a faster convergence speed and better convergence effect than those of particle swarm optimization. Therefore, the upper optimization in this article adopts the `fmincon` function to solve the nonlinear programming problem. As the IESs at the lower level have the power interaction relationship and are not independent of each other, it is difficult to solve the single objective optimization algorithm, so this article uses the multi-objective optimization algorithm for the optimization of the lower level IESs.

The multi-objective particle swarm algorithm was first proposed by Carlos a. Coello Coello et al. in 2004. Its role is to apply the particle swarm algorithm, originally used only for the single-objective problem, to the multi-objective problem by introducing Pareto dominance [31], [32]. Multi-objective particle swarm optimization (MOPSO) is better on the iterative speed and effect than the second generation of the non-dominated sorting genetic algorithm (NSGA-II), so this article selects the multi-objective particle swarm algorithm to optimize the lower level.

The specific optimization steps of the lower scheduling model are as follows:

- 1) Input the parameters of the lower IESs to generate the population formed by the interactive power of each IES.
- 2) According to the exchange power between the distribution network and each IES and the interactive power between each IES, the output of each equipment piece in the IES is obtained, the objective function value of the particle is calculated, the optimal position of the particle individual is determined, and the non-inferior solution is stored in the external particle swarm.
- 3) Determine the historical optimal solution of each particle and the global optimal solution of the population.
- 4) Update the velocity and position of each particle. The objective function value of each particle is calculated, the historical optimal solution of the particle is updated according to the dominant relationship, and a new set of non-inferior solutions is formed.
- 5) Update the non-inferior solution set and select the global optimal solution.
- 6) Determine whether the maximum number of iterations is reached. If so, then the optimal Pareto solution is output, and a group of particles with the lowest total cost is selected and transmitted to the upper level. Otherwise, return to step (4).

The solution process of the bi-level optimal scheduling model is shown in Figure 4.

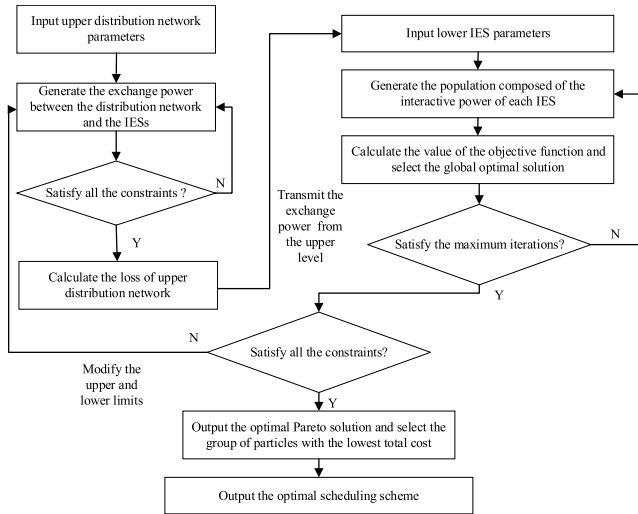


FIGURE 4. Process of solving the bi-level optimal scheduling model.

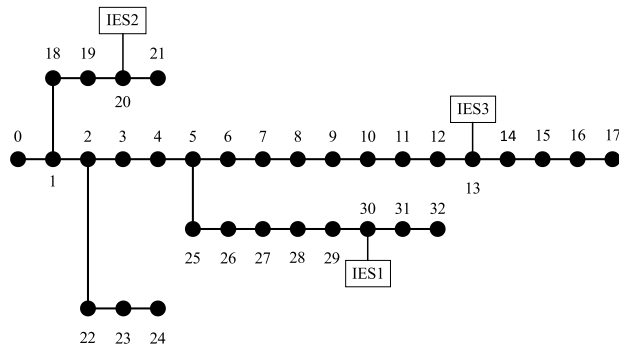


FIGURE 5. Structure of the IEEE 33-node distribution system.

IV. CASE STUDIES

A. OPTIMAL RESULTS IN THE FIRST STAGE

In this article, the IEEE 33-node distribution system is used for example analysis, and a typical winter day in a region in South China is selected as a regional optimal scheduling scenario. Nodes 13, 20 and 30 of a distribution network are connected to an industrial area (IES3), commercial area (IES2) and residential area (IES1), respectively. It is assumed that the stakeholders of each IES in the region are different, as shown in Figure 5. Among them, the park-level integrated energy systems share the same CCHP structure, but the capacity of the equipment is different.

First, considering the demand response, the electricity price of each IES before and after the demand response is shown in Table 1. The electric quantity of each IES is shown in Figures 6-8.

The schedulable potential of each IES is shown in Figure 9. A negative value of the schedulable potential means the IES sells electricity to the grid. For IES1, as the energy demand of the residential users does not fluctuate substantially and the maximum output value of the gas turbine is small, the absolute value of the overall schedulable potential remains below 1000 kW. At 21 h, each IES is in the peak

TABLE 1. Electricity price of each IES before and after the demand response.

Area	Before demand response(¥ /kWh)	After demand response(¥ /kWh)		
		Peak	Off-peak	Valley
Residential area	0.5283	0.8572	0.5316	0.2703
Commercial area	0.6715	0.7586	0.5426	0.2000
Industrial area	0.6465	0.7733	0.6285	0.3985

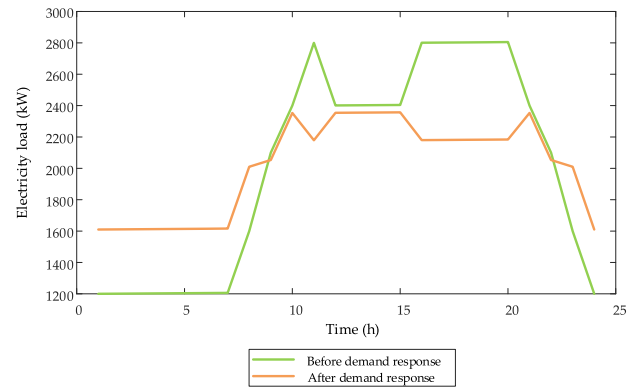


FIGURE 6. Electric quantity before and after the demand response in the residential area.

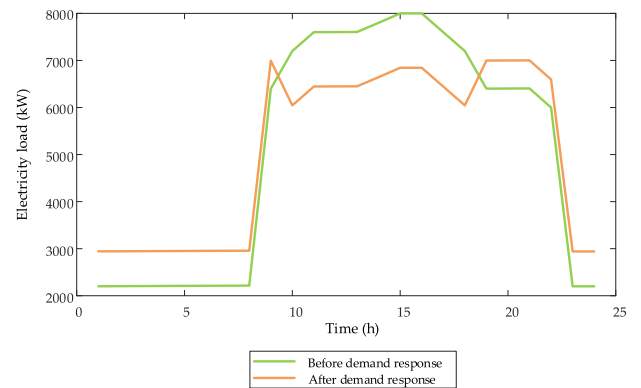


FIGURE 7. Electric quantity before and after the demand response in the commercial area.

of power consumption, at which time the absolute value of IES1 schedulable potential reaches the minimum value. For IES2, during the 23-8 h, IES2 has a large output value as an equivalent power source to prevent the voltage of the distribution network out of limit. At 8 h, the power consumption of each IES has not reached the peak yet, and photovoltaic power is supplied to the IESs at the same time, so IES2 has the maximum absolute value of schedulable potential. During the 9-22 h period, the commercial area has a large demand for energy, so the schedulable potential curve shows an obvious

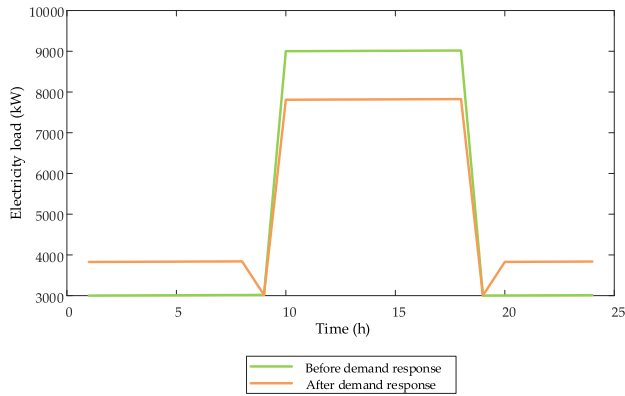


FIGURE 8. Electric quantity before and after the demand response in the industrial area.

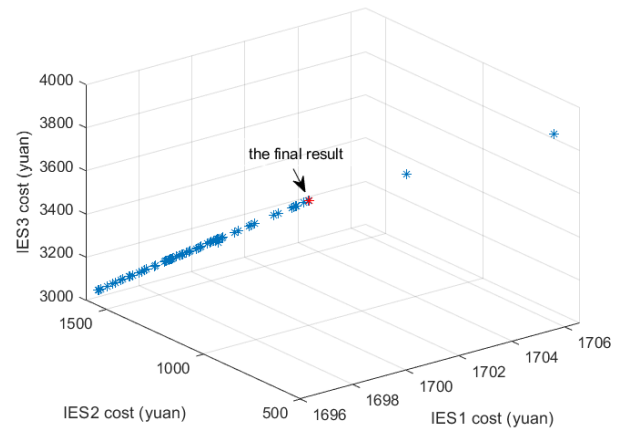


FIGURE 10. Pareto frontier.

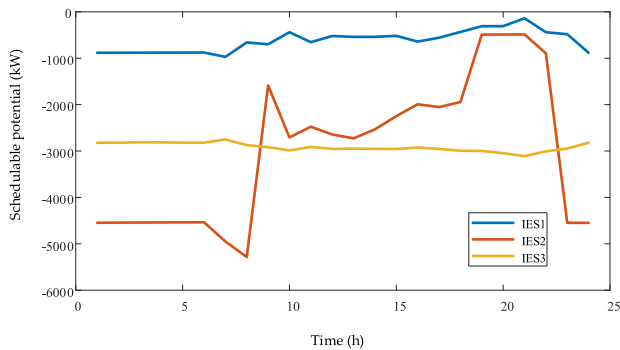


FIGURE 9. Schedulable potential of each IES.

upward trend. At the same time, because there is no photovoltaic output during 19-22 h, the absolute value of the schedulable potential of IES2 reaches the valley value at this stage. For IES3, there is no obvious variation trend of schedulable potential curve in the peak period due to the limitation of distribution network security. During the 10-18 h peak period of power consumption, because of the large energy demand of the IES itself, the schedulable potential is maintained in a relatively stable state.

B. BI-LEVEL SCHEDULING OPTIMIZATION RESULTS IN THE SECOND STAGE

According to the electricity price and electricity quantity of each IES obtained in the first stage, a bi-level optimal scheduling model is established. The IESs purchase and sell electricity from the distribution network through the tie-line. Meanwhile, the IESs also interact with each other through the tie-line, ignoring the energy loss in the process of energy interaction. In this article, the electricity price of the power grid is set as 0.8-fold the electricity price of the power purchase, and the electricity price bought and sold between IESs is 0.8-fold the electricity price sold from an IES to the power grid.

According to the model described in Section III, the optimal scheduling scheme of each IES is obtained. Taking the 4 h scheduling scheme as an example, the particle number is set as 50, the inertia factors are set as 0.9 and 0.4 respectively,

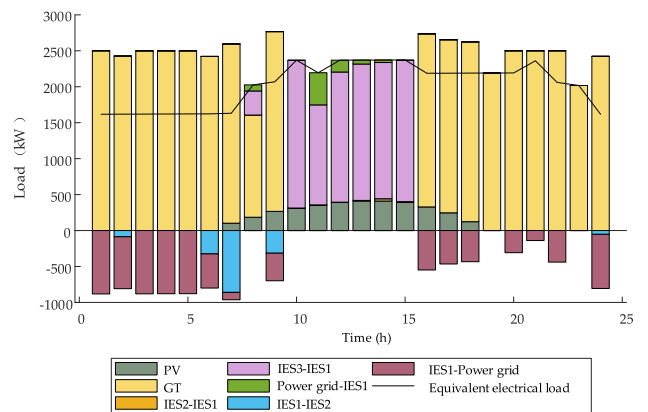


FIGURE 11. IES1 electrical energy distribution results.

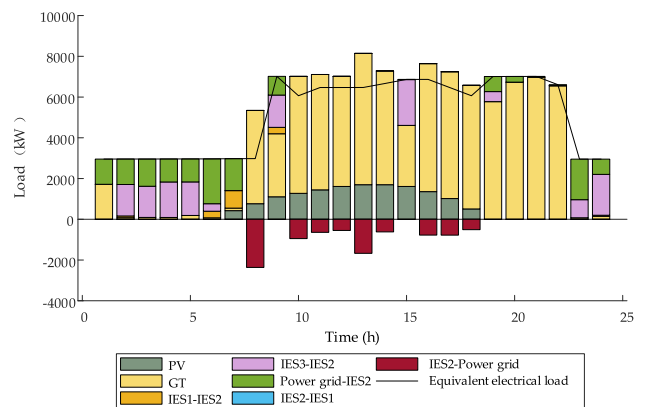


FIGURE 12. IES2 electrical energy distribution results.

and two learning factors are both set as 2. When the iteration times are 100, Pareto frontier is basically fixed, and a better solution can be obtained. Pareto frontier obtained is shown in Figure 10. There is no absolute optimal solution for Pareto optimal. In this article, the solution with the lowest total cost is selected as the optimal solution.

The day-ahead scheduling power distribution results of each IES are shown in Figures 11-13, and the thermal energy distribution results are shown in Figures 14-16. The

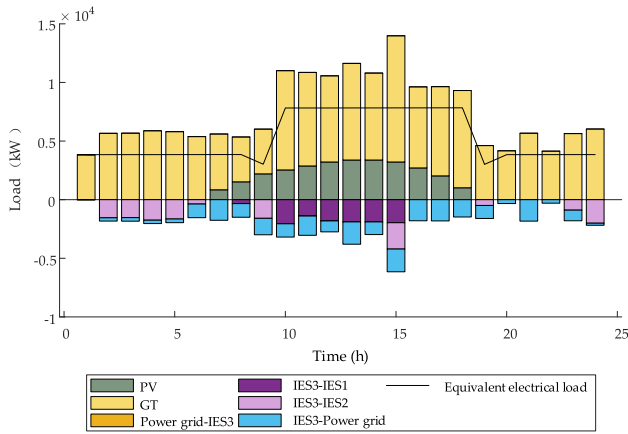


FIGURE 13. IES3 electrical energy distribution results.

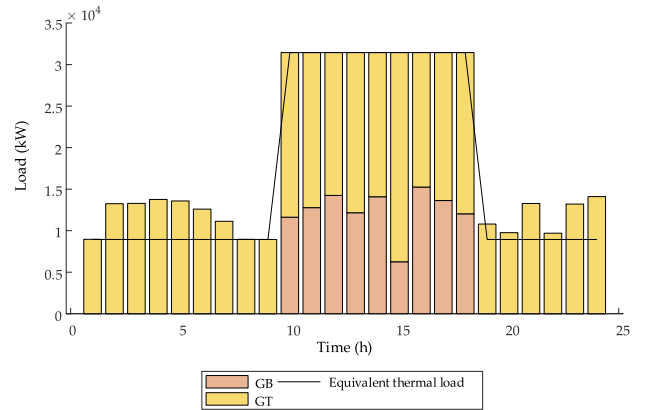


FIGURE 16. IES3 thermal energy distribution results.

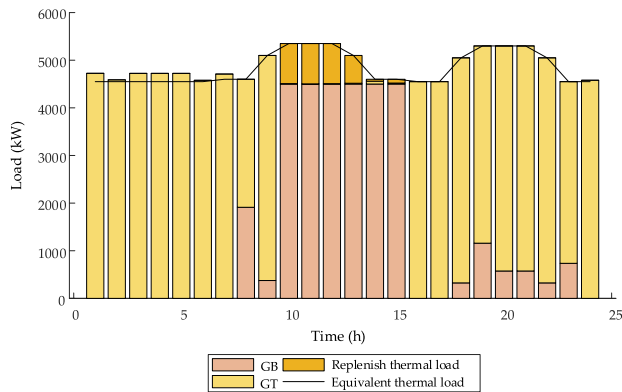


FIGURE 14. IES1 thermal energy distribution results.

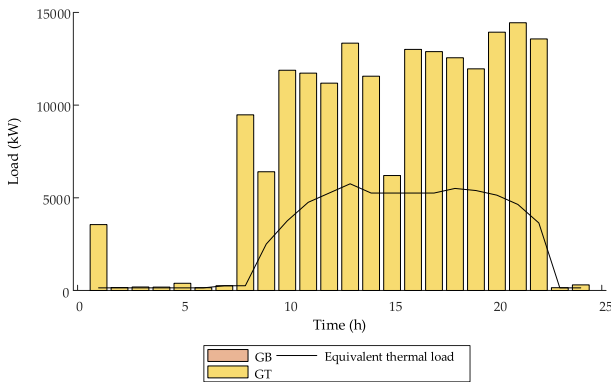


FIGURE 15. IES2 thermal energy distribution results.

equivalent electrical load is defined as the sum of the user’s electricity load and the electrical energy demand of the electric chiller. The equivalent thermal load is defined as the sum of the user’s thermal load and the thermal energy demand of the absorption chiller. Here, positive power represents the energy supply, and negative power represents energy consumption.

Figures 11-13 show that, for IES1, because of the small power load demand of the IES itself, the electricity demand is mostly met by gas turbines and photovoltaic power

generation. The excess electricity is sold to the power grid to prevent the power grid voltage from exceeding the limit. For IES2, the electricity demand is usually met by IES3 and the grid during the valley period. In the peak period, IES2 increases the gas turbine output, and the excess electricity is sold to the grid as equivalent power output. For IES3, gas turbines and photovoltaic power generation are primarily used in the IES. In the valley period, most of the excess electricity is sold to IES2, and a small part of the electricity is sold to the power grid, which reduces the cost of IES2 while preventing too much electricity from being sold to the power grid and improving the safety of the distribution network. In the peak period, as there is a large demand for heat in the IES, the demand is primarily met by gas turbines and photovoltaic power generation, and the surplus electricity is sold to IES1 and the distribution network.

Figures 14-16 show that, for IES1, the gas boiler provides thermal energy only during the peak period and after the gas turbine output is limited. When the output of the gas boiler is limited, there will be a small amount of vacancy, which can be supplemented by purchasing heat from IES2 or the heating network. For IES2, gas turbine heat generation can meet the equivalent thermal load demand due to a small thermal load demand in the commercial area. At the same time, because the method of fixing power based on heat is adopted in this article, the heat production will be greater than the equivalent heat load. For IES3, because the industrial area has a large demand for thermal load at 10-18 h, the waste heat generated by the gas turbine cannot meet the thermal load demand in the industrial area, and it is supplemented by the gas boiler at this time.

C. COMPARISON OF DIFFERENT SCHEDULING MODES

Scheme 1: The IESs do not participate in the distribution network scheduling.

Scheme 2: The IESs participate in the scheduling of the distribution network without one-stage optimization.

Scheme 3: The two-stage optimal scheduling model proposed in this article.

Table 2 shows that, when the IESs do not participate in the scheduling of the distribution network, the IESs take the

TABLE 2. Comparison of different scheduling modes.

Scheme	Is the voltage out of limit?	Total network loss /MW	Total cost / $\times 10^4$ ¥
1	Yes	17.5234	22.4789
2	No	4.3740	23.8326
3	No	3.6298	22.5546

TABLE 3. The situation of the voltage out of limit in scheme 1.

Node	Average voltage deviation rate	Node	Average voltage deviation rate	Node	Average voltage deviation rate
6	9.44%	13	17.97%	27	9.67%
7	10.22%	14	19.52%	28	10.29%
8	12.56%	15	19.45%	29	10.73%
9	10.36%	16	19.39%	30	10.89%
10	12.86%	17	19.29%	31	9.10%
11	13.44%	18	19.27%	32	9.17%
12	13.76%	26	9.54%	33	9.20%

minimum cost as the only goal, sacrificing the security of the distribution network and resulting in a large total loss of lines. In the peak period of 10-20 h, the voltage of some nodes will be out of limit. The degree of the voltage out of limit is represented by the average voltage deviation rate in Table 3. When IESs participate in the distribution network scheduling, but do not perform a phase of optimization, the total loss of the line and the total cost are higher; compared with scheme 2, the total loss of the line is reduced by 17.01% and the total cost by 5.36%. The security of the distribution network is guaranteed and the loss of the network is reduced, while the total cost in the IESs is reduced, realizing a win-win situation between the distribution network and the IESs.

V. CONCLUSION

In this article, a two-stage joint optimal scheduling model of a distribution network with IESs is established. The following conclusions can be drawn through an example of park-level integrated energy systems in a certain region:

- 1) When the IES is connected to the distribution network, it acts as an equivalent power source. When there is excess electrical energy in the IES, it will transmit electrical energy to the distribution network to reduce the loss of the distribution network; when there is too much excess electrical energy in the IES, energy interaction will be conducted among the IESs to prevent the voltage of the distribution network from exceeding the limit.
- 2) The IES with excess electricity can determine the distribution of excess electricity according to the current electricity price. Because of the interest relationship between each IES, they are not independent. The multi-objective optimization method adopted in this article can effectively ensure the economic efficiency of each IES.

- 3) Compared with the two schemes in which the IESs do not participate in the scheduling and the IESs participate in the scheduling but do not perform the one-stage optimization, the two-stage joint optimal scheduling method of the distribution network with IESs proposed in this article effectively reduces the loss of the distribution network and ensures the safe and reliable operation of the distribution network. At the same time, the total cost of the IESs is reduced during the scheduling period, which verifies the reliability and economy of the model proposed in this article.

In fact, there are still some limitations and deficiencies in this article. On the one hand, for the IESs with low demand for electric energy and high demand for thermal energy, the fixing power based on heat method adopted in this article may lead to low schedulable potential, thus exerting a certain influence on the following two-layer optimal scheduling. On the other hand, this article only considers a part of the output equipment in the IES and does not consider the influence of the energy storage devices on the schedulable potential of the IES. In the future, the problem of optimal scheduling of the distribution network with IESs including energy storage devices will be further studied to improve the practicality of the optimal scheduling model.

REFERENCES

- [1] M. A. Hannan, M. Faisal, P. J. Ker, L. H. Mun, K. Parvin, T. M. I. Mahlia, and F. Blaabjerg, "A review of Internet of energy based building energy management systems: Issues and recommendations," *IEEE Access*, vol. 6, pp. 38997–39014, 2018.
- [2] E. A. Martinez Cesena and P. Mancarella, "Energy systems integration in smart districts: Robust optimisation of multi-energy flows in integrated electricity, heat and gas networks," *IEEE Trans. Smart Grid*, vol. 10, no. 1, pp. 1122–1131, Jan. 2019.
- [3] C. Acosta, M. Ortega, T. Bunsen, B. Koirala, and A. Ghorbani, "Facilitating energy transition through energy commons: An application of socio-ecological systems framework for integrated community energy systems," *Sustainability*, vol. 10, no. 2, p. 366, Jan. 2018.
- [4] M. Nazari-Heris, B. Mohammadi-Ivatloo, and S. Asadi, "Optimal operation of multi-carrier energy networks considering uncertain parameters and thermal energy storage," *Sustainability*, vol. 12, no. 12, p. 5158, Jun. 2020.
- [5] K. Zhang, Y. Ding, H. Hui, X. Fang, and K. Xie, "Dispatching potential evaluation of thermostatically controlled loads based on realistic customer electricity data in China," in *Proc. IEEE 3rd Conf. Energy Internet Energy Syst. Integr. (EI2)*, Nov. 2019, pp. 589–593.
- [6] X. Feng, G. Lin, Q. Xu, S. Lu, and T. Xie, "Bi-level dynamic optimization dispatch decision method for cluster air-conditioning loads," *Electr. Power Autom. Equip.*, vol. 40, no. 6, pp. 29–36, 2020.
- [7] W. Huang, P. Xiong, L. Hua, L. Liu, and Z. Liu, "Multi-Objective optimization dispatch of active Distribution network based on dynamic schedule priority," *Trans. China Electrotech. Soc.*, vol. 33, no. 15, pp. 3486–3489, 2018.
- [8] T. Yi, X. Cheng, Y. Chen, and J. Liu, "Joint optimization of charging station and energy storage economic capacity based on the effect of alternative energy storage of electric vehicle," *Energy*, vol. 208, Oct. 2020, Art. no. 118357.
- [9] Y. Wang, Y. Wang, Y. Huang, F. Li, M. Zeng, J. Li, X. Wang, and F. Zhang, "Planning and operation method of the regional integrated energy system considering economy and environment," *Energy*, vol. 171, pp. 731–750, Mar. 2019.
- [10] R. S. Patwal and N. Narang, "Multi-objective generation scheduling of integrated energy system using fuzzy based surrogate worth trade-off approach," *Renew. Energy*, vol. 156, pp. 864–882, Aug. 2020.

- [11] M. Li, Y. Feng, M. Zhou, H. Mu, L. Li, and Y. Wang, "Economic and environmental optimization for distributed energy system integrated with district energy network," *Energies*, vol. 12, no. 10, p. 1844, May 2019.
- [12] P. Li, Z. Wang, L. Hou, Y. Yin, Y. Liu, and X. Zhang, "Analysis of repeated game based optimal operation for regional integrated energy system," *Autom. Electr. Power Syst.*, vol. 43, no. 14, pp. 81–89, 2019.
- [13] W. Lin, X. Jin, Y. Mu, H. Jia, X. Xu, X. Yu, and B. Zhao, "A two-stage multi-objective scheduling method for integrated community energy system," *Appl. Energy*, vol. 216, pp. 428–441, Apr. 2018.
- [14] J. Tan, Q. Wu, Q. Hu, W. Wei, and F. Liu, "Adaptive robust energy and reserve co-optimization of integrated electricity and heating system considering wind uncertainty," *Appl. Energy*, vol. 260, Feb. 2020, Art. no. 114230.
- [15] D. Wang, Y. Zhi, B. Yu, Z. Chen, Q. An, L. Cheng, and M. Fan, "Optimal coordination control strategy of hybrid energy storage systems for tie-line smoothing services in integrated community energy systems," *CSEE J. Power Energy Syst.*, vol. 4, no. 4, pp. 408–416, Dec. 2018.
- [16] Y. Jiang, J. Xu, Y. Sun, C. Wei, J. Wang, S. Liao, D. Ke, X. Li, J. Yang, and X. Peng, "Coordinated operation of gas-electricity integrated distribution system with multi-CCHP and distributed renewable energy sources," *Appl. Energy*, vol. 211, pp. 237–248, Feb. 2018.
- [17] Y. Zhong, H. Zhou, X. Zong, Z. Xu, and Y. Sun, "Hierarchical multi-objective fuzzy collaborative optimization of integrated energy system under off-design performance," *Energies*, vol. 12, no. 5, p. 830, Mar. 2019.
- [18] M. Hemmati, M. Abapour, B. Mohammadi-Ivatloo, and A. Anvari-Moghaddam, "Optimal operation of integrated electrical and natural gas networks with a focus on distributed energy hub systems," *Sustainability*, vol. 12, no. 20, p. 8320, Oct. 2020.
- [19] Y. Wang, Y. Ma, F. Song, Y. Ma, C. Qi, F. Huang, J. Xing, and F. Zhang, "Economic and efficient multi-objective operation optimization of integrated energy system considering electro-thermal demand response," *Energy*, vol. 205, Aug. 2020, Art. no. 118022.
- [20] H. Yang, M. Li, Z. Jiang, and P. Zhang, "Multi-time scale optimal scheduling of regional integrated energy systems considering integrated demand response," *IEEE Access*, vol. 8, pp. 5080–5090, 2020.
- [21] M. Geidl, *Integrated Modeling and Optimization of Multi-Carrier Energy Systems*. Zürich, Switzerland: ETH Zürich, Swiss Federal Institute of Technology Zurich, 2007, pp. 23–75.
- [22] M. Geidl and G. Andersson, "Optimal power flow of multiple energy carriers," *IEEE Trans. Power Syst.*, vol. 22, no. 1, pp. 145–155, Feb. 2007.
- [23] F. Kienzle, P. Ahefn, and G. Andersson, "Valuing investments in multi-energy conversion, storage, and demand-side management systems under uncertainty," *IEEE Trans. Sustain. Energy*, vol. 2, no. 2, pp. 194–202, Apr. 2011.
- [24] M. C. Bozchalui, S. A. Hashmi, H. Hassen, C. A. Canizares, and K. Bhattacharya, "Optimal operation of residential energy hubs in smart grids," *IEEE Trans. Smart Grid*, vol. 3, no. 4, pp. 1755–1766, Dec. 2012.
- [25] M. A. Mirzaei, M. Z. Oskouei, B. Mohammadi-Ivatloo, A. Loni, K. Zare, M. Marzband, and M. Shafiee, "Integrated energy hub system based on power-to-gas and compressed air energy storage technologies in the presence of multiple shiftable loads," *IET Gener., Transmiss. Distrib.*, vol. 14, no. 13, pp. 2510–2519, Jul. 2020.
- [26] A. Garulli, S. Paoletti, and A. Vicino, "Models and techniques for electric load forecasting in the presence of demand response," *IEEE Trans. Control Syst. Technol.*, vol. 23, no. 3, pp. 1087–1097, May 2015.
- [27] H. A. Aalami, M. P. Moghaddam, and G. R. Yousefi, "Demand response modeling considering interruptible/curtailable loads and capacity market programs," *Appl. Energy*, vol. 87, no. 1, pp. 243–250, Jan. 2010.
- [28] K. McKenna and A. Keane, "Residential load modeling of price-based demand response for network impact studies," *IEEE Trans. Smart Grid*, vol. 7, no. 5, pp. 2285–2294, Sep. 2016.
- [29] H. Abdi, E. Dehnavi, and F. Mohammadi, "Dynamic economic dispatch problem integrated with demand response (DEDDR) considering non-linear responsive load models," *IEEE Trans. Smart Grid*, vol. 7, no. 6, pp. 2586–2595, Nov. 2016.
- [30] H. T. Nguyen, A. S. Al-Sumaiti, K. Turitsyn, Q. Li, and M. S. El Moursi, "Further optimized scheduling of micro grids via dispatching virtual electricity storage offered by deferrable power-driven demands," *IEEE Trans. Power Syst.*, vol. 35, no. 5, pp. 3494–3505, Sep. 2020.
- [31] C. A. C. Coello, G. T. Pulido, and M. S. Lechuga, "Handling multiple objectives with particle swarm optimization," *IEEE Trans. Evol. Comput.*, vol. 8, no. 3, pp. 256–279, Jun. 2004.
- [32] A. Elgammal and M. El-Naggar, "Energy management in smart grids for the integration of hybrid wind-PV-FC-battery renewable energy resources using multi-objective particle swarm optimisation (MOPSO)," *J. Eng.*, vol. 2018, no. 11, pp. 1806–1816, Nov. 2018.



YUHAN JIANG received the B.S. degree in electrical engineering from the School of Electrical and Electronic Engineering, Hubei University of Technology (HBUT), Wuhan, China, in 2019. She is currently pursuing the M.S. degree with the College of Energy and Electrical Engineering, Hohai University. Her research interests include renewable energy power generation technology and integrated energy system optimal operation.



FEI MEI (Member, IEEE) received the Ph.D. degree from the School of Electrical Engineering, Southeast University (SEU), Nanjing, China, in 2014. He is currently a Lecturer with the College of Energy and Electrical Engineering, Hohai University (HHU), Nanjing. His research interests include artificial intelligence technology in power systems, renewable energy power generation technology, online monitoring and fault diagnosis for power equipment, and integrated energy system optimal operation.



JIXIANG LU is currently a Senior Engineer with the State Key Laboratory of Smart Grid Protection and Control, NARI Group Corporation, Nanjing, China. His research interest includes renewable energy power generation technology.



JINJUN LU is currently a Senior Engineer with the State Key Laboratory of Smart Grid Protection and Control, NARI Group Corporation, Nanjing, China. His research interest includes renewable energy power generation technology.

• • •